

# Using Ultracapacitors as Energy-storing Devices on a Mobile Robot Platform Power System for Ultra-fast Charging

Carlos Arantes<sup>1</sup>, João Sepúlveda<sup>2</sup>, João Sena Esteves<sup>2</sup>, Hugo Costa<sup>1</sup> and Filomena Soares<sup>2</sup>

<sup>1</sup>Department of Industrial Electronics, University of Minho, Campus of Azurém, 4800-058 Guimarães, Portugal

<sup>2</sup>Centre Algoritmi, Department of Industrial Electronics, University of Minho, Campus of Azurém, 4800-058 Guimarães, Portugal

**Keywords:** Ultracapacitors, Batteries, Fast Electric Charger, Mobile Robot.

**Abstract:** The large charging times required by conventional batteries constitute an important limitation in many applications. The use of ultracapacitors as energy storage elements allows substantially faster charging. This paper presents a power supply system developed in order to validate the possibility of providing a mobile robot platform with an electrical energy storage system based on ultracapacitors and batteries, ensuring both the autonomy and the charging time required by this vehicle. Both simulations results and experimental results – also presented in this paper – validate this possibility. Using exclusively one ultracapacitors module as energy-storing device of the new power supply system, the mobile platform achieved an autonomy of 22 minutes after a charging time of 1 minute and 57 seconds. The charging time is less than 10% of the autonomy time. The system also proved its ability to properly charge lead-acid batteries or nickel–metal hydride batteries, which may be used as energy-storing devices, allowing the mobile platform to achieve greater autonomy than the one obtained with ultracapacitors (at the cost of larger charging times).

## 1 INTRODUCTION

Conventional batteries usually require charging times of, at least, some tens of minutes due to the allowable values of their charging currents. These charging times are an important limitation in many applications, such as electric vehicles. Although many authors proposed battery fast charging techniques for different battery types (Petchjaturorn, 2005; Li, 2009; Hua, 2010), charging times cannot be reduced much further, because the temperature rises too much, deteriorating the batteries.

The charging currents of ultracapacitors may be substantially higher than those allowed by common batteries. So, ultracapacitors charging periods may be much smaller than those required by batteries. This paper addresses the possibility of using ultracapacitors as energy-storing devices when very reduced charging times are required.

Since batteries have much higher energy densities than ultracapacitors, they are more suitable to store large amounts of energy in order to provide a large autonomy to onboard powered devices. Regarding this aspect, the difference between batteries and ultracapacitors may be substantially

reduced in a near future due to the introduction of new materials (Bernholc, 2010).

The discharging currents of ultracapacitors may also be substantially higher than those allowed by common batteries. Due to this fact, ultracapacitors are able to provide power peaks of significant value. Several applications integrating batteries and ultracapacitors on the same system are currently available (Schneuwly, 2000; Wenzhong, 2005; Miller, 2007; Awerbuch, 2008; Xiaofei, 2009; Awerbuch, 2010; Dai, 2010; Haihua, 2010; Lei, 2010; Niemoeller, 2010; JennHwa, 2011; Monteiro, 2011; Musat, 2012). This integration results from the need of having a single system capable of, simultaneously:

1. Storing large amounts of energy in the batteries for the sake of autonomy;
2. Providing power peaks of short duration but significant value using the ultracapacitors, extending the battery lifetime (Musat, 2012) and/or ensuring the proper functioning of the system (Schneuwly, 2000; Monteiro, 2011).

This paper also addresses the possibility of integrating batteries and ultracapacitors in the same device. However, the main reason for doing so is different from the previously described. Having

batteries released from the requirement of providing high power peaks remains an important property of a power supply system. But the main goal of the integration suggested in this paper is enabling a vehicle to achieve a reasonable autonomy after a very reduced charging time, when its energy-storing devices (batteries and ultracapacitors) become discharged and there is not enough time to properly charge the batteries.

The main objective of the power supply system presented in this paper is to validate the possibility of providing a mobile robot platform with an electrical energy storage system based on ultracapacitors and batteries, ensuring both the autonomy and the charging speed required by this vehicle. Starting with fully discharged energy-storing devices, the mobile platform must achieve, at least

1. 15 minutes of autonomy after a charging period not exceeding 2 minutes, when there is not more time available for charging;
2. Some hours of autonomy, when there are no charging time restrictions.

Conventional batteries easily accomplish the second task. For example, the expected autonomy of the mobile platform powered by a fully charged 12V, 12Ah, 144Wh lead-acid battery ranges from 7 to 9 hours.

So, the main effort was put on studying the possibility of accomplishing the first task using only ultracapacitors. That is the reason why the majority of the results presented in this paper are related to the use of one 16V, 116F, 4.12Wh ultracapacitors module. Since batteries are not used in the first task, this paper may be put in the context of “environmental-friendly” approaches.

Conventional batteries are, still, much less expensive than ultracapacitors. However, ultracapacitors cost has been significantly decreasing. For example, the cost of the ultracapacitors module used in this work decreased 34% in a period of about one year. By now, it costs 4.3 times more than the 12V, 12Ah, 144Wh lead-acid battery also used in this work.

On the other hand, ultracapacitors allow about 1000 times more charging/discharging cycles than batteries. The rated number of cycles between rated voltage and half rated voltage (under constant current at 25°C) allowed by the previously mentioned ultracapacitors module is 500000.

The energy-storing device of the new power supply system, described in Section 2, may be an ultracapacitors module or a battery. Future versions

of the system will integrate energy-storing devices of both kinds.

Section 3 presents simulation results performed before implementing the physical system described in Section 4. Some experimental results obtained with the real system are presented in Section 5. The general conclusions and some considerations regarding future developments are provided in Sections 6.

## 2 SYSTEM ARCHITECTURE OVERVIEW

The developed power supply system has three components:

- **An energy-storing device**, which may be an ultracapacitors module, a lead-acid battery or a nickel–metal hydride battery;
- **A charger**, intended to transfer energy from the mains to the energy-storing device;
- **A voltage regulator**, intended to supply a regulated voltage to the mobile robot platform, regardless of the voltage of the energy-storing device.

### 2.1 The Charger

Figure 1 shows the block diagram of the subsystem that uses the charger. The energy-storing device may be an ultracapacitor (or an ultracapacitors module, like the 16V, 116F, 4.12Wh module used in this work). The charger is also appropriate for lead-acid batteries or nickel-metal hydride batteries.

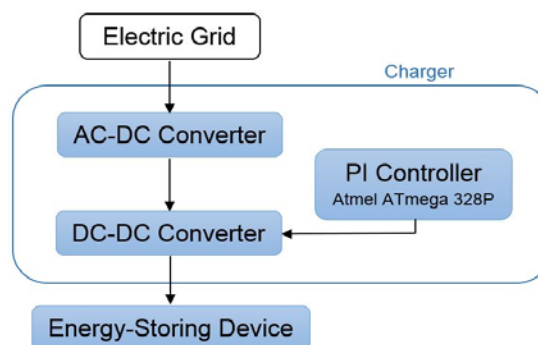


Figure 1: Block diagram of the subsystem that uses the charger.

In the majority of European countries, the characteristics of single-phase standard electric plugs are 230V AC, 50Hz and 16A (3.45kVA). The charger circuit is fed by a 1.5kVA, 50Hz, 230V to

18V single phase transformer, followed by a 25A rectifier bridge and a 25mF capacitive filter. A 5W, 10Ω resistor is connected in series with the filtering capacitors, to avoid a large start up surge in the electric current. Two seconds later, the resistor is bypassed by a timer relay. This results in an unregulated 24V DC power supply, which feeds a power electronics converter, with a permitted ripple of 5V and a rated power of 300W.

The power electronics converter of the charger is a step-down DC-DC converter working with pulse width modulation current-controlled voltage source, at a switching frequency of 9.7kHz. The input is a non-regulated 24V DC voltage and the output is a regulated adjustable DC current. The control system is a PI (proportional + integral) controller with a sampling frequency of 1kHz, with a proportional gain ( $K_p$ ) of 8.2 and an integral gain ( $K_i$ ) of 10. Figure 2 shows the step-down model developed with PSIM simulation software.

In the converter shown in Figure 2, diode D5 ensures that the energy always flows one way, towards the battery or the ultracapacitors module. Diode D6, resistor R17 and capacitor C10 form a RCD snubber whose goal is to mitigate the overvoltages that occur when the MOSFET is turned off. Regarding snubber parameters calculation, a maximum current of 20A and a parasitic system inductance of 100nH were considered. In this situation, capacitor C10 (150nF, 100V) must be capable of absorbing the energy stored in the parasite coil through D6 and discharged through resistor R17 (1Ω, 5W). Capacitor C4 (10μF, 100V) is a polypropylene capacitor that also contributes to the mitigation of overvoltages.

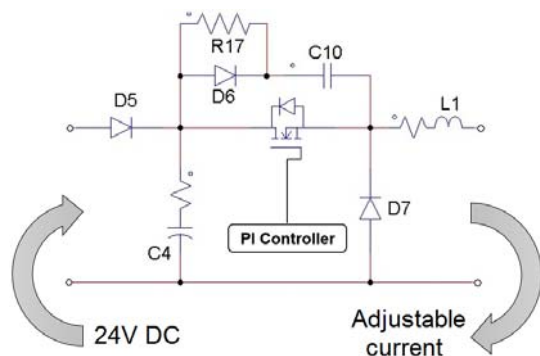


Figure 2: PSIM model of the step-down converter of the charger.

L1 is the output filter coil (14.6mH, 170mΩ at 1 kHz) that allows smoothing the current around an average adjustable value. D7 is a diode that ensures the path to the current when the MOSFET is turned

off. The diodes used are the schottky MBR1660 and the MOSFET used is the P80PF55.

## 2.2 The Voltage Regulator

Figure 3 shows the block diagram of the subsystem that uses the voltage regulator. The objective of this component is to supply energy to the mobile robot platform from the energy previously stored in the battery or in the ultracapacitors module.

The main characteristics of the load (mobile robot platform) are a nominal voltage of 12V and a maximum power of 30W. Since the power supplied to the mobile platform is mainly used to drive DC motors, the voltage *ripple* is not a very relevant issue.

Unlike a battery voltage, which is reasonably constant during discharging process, a capacitor voltage is directly proportional to its charge, causing a large variation on its voltage when it supplies a load. So, when the ultracapacitors module is used as energy-storing device, a voltage regulator is required in order to keep the load voltage set to the intended value of 12V independently of the ultracapacitors module voltage.

The voltage regulator also allows using different types of batteries, with different rated voltages.

The voltage regulator consists of two DC-DC converters: a step-up followed by a step-down. This topology was preferred over the step-up/down topology because, in that case, the output voltage would have reversed polarity in relation to the input voltage, and this would require the use of isolated voltage sensors for measuring. With the implemented topology, the measurement is carried out using a simple resistive voltage divider.

The step-down sub-circuit maintains the output voltage set on the intended value as long as the input voltage remains above that value. When the input voltage becomes lower than the output intended value, the step-up sub-circuit elevates it to the output intended value. There are still situations when none of the sub-circuits operate as DC-DC converters, as is the case in which the input voltage is between 13V and 12.5V. In this case, the step-up MOSFET stays off while the step-down MOSFET stays on. This results in a varying output voltage but, in practice, the effect is negligible.

The two converters never switch simultaneously, as this would entail unnecessary additional power losses. Figure 4 shows the voltage regulator model developed with PSIM simulation software.

In Figure 4, diode D1 ensures that the energy only flows from the input to the output. Diode D2

provides a path for the current when the MOSFET belonging to the step-up sub-circuit is open. L1 is a coil belonging to the step-up sub-circuit, with an inductance of 168.7 $\mu$ H and a resistance of 170m $\Omega$  at 1kHz. L2 is a coil belonging to step-down sub-circuit and has an inductance of 132.4 $\mu$ H and a resistance of 148m $\Omega$  at 1kHz. Capacitors C1 and C2, both of 1mF, form capacitive filters that are intended to minimize the ripple caused by high switching frequencies of both MOSFETs.

The control algorithm consists of a PI controller with proportional gain of 1 and integral gain of 10 runs the control algorithms of both sub-circuits. The input voltage, read through one of the channels of the microcontroller ADC, allows the selection of the sub-circuit to be switched at any moment. The main control cycle runs at a frequency of 1kHz, while semiconductors (MOSFETs) switch at a frequency of 7.8kHz.

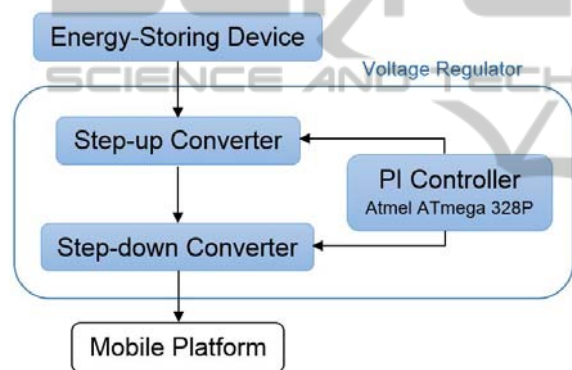


Figure 3: Block diagram of the subsystem that uses the voltage regulator.

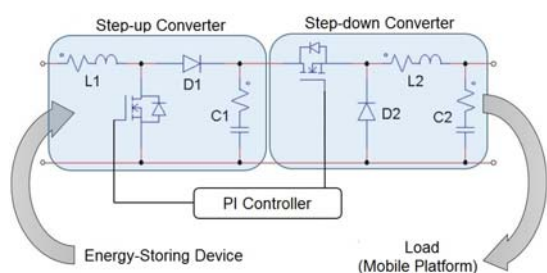


Figure 4: PSIM model of the DC-DC converters of the voltage regulator.

### 3 SIMULATION RESULTS

The PSIM simulation software was used to validate all the developed blocks of the entire system, before any circuit implementation and execution of any experimental tests.

The simulations results also made possible making minor adjustments to the controller gains, allowing a better performance.

The most important simulations results are presented in this section.

#### 3.1 The Charger

The charger was simulated when feeding an 116F ultracapacitor. A reference current of 20A and a final voltage of 15V were considered. Figure 5 shows that the ultracapacitor charging is performed successfully.

#### 3.2 The Voltage Regulator

The voltage regulator was simulated considering an 116F ultracapacitor charged up to 15V, supplying a 12V, 2A load. In Figure 6, it is visible that the circuit draws more current from the ultracapacitor as its voltage drops, in order to maintain constant the output power.

In Figure 7, the load current and voltage are shown, when the voltage regulator is fed by a 116F ultracapacitor previously charged up to 15V. Load voltage and current values remain approximately constant, except on a very short time period around the 190th second, when slight drops in both voltage and current are observed. This is due to an input voltage interval where none of the DC-DC converters – step-up or step-down – is switching, in order to improve energy efficiency. However, these small drops do not disturb the proper functioning of the mobile platform.

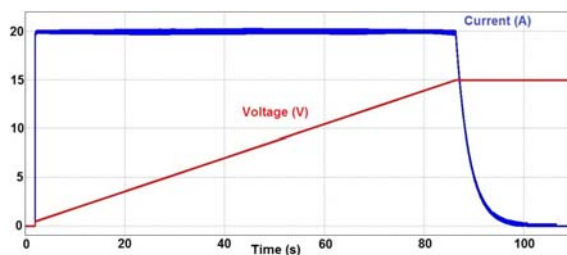


Figure 5: PSIM simulation results of the charger when charging an 116F ultracapacitor up to 15V.

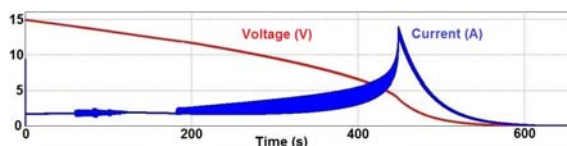


Figure 6: PSIM simulation results of an 116F ultracapacitor voltage and current, when the regulator feeds a 12V, 2A load.

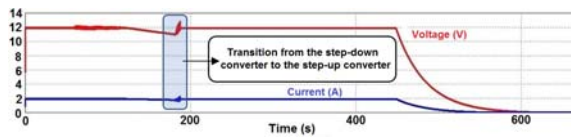


Figure 7: PSIM simulation results of load voltage and current when an 116F ultracapacitor feeds the voltage regulator.

## 4 SYSTEM IMPLEMENTATION

In this section, a detailed description of the real system implementation is made. The implementation was performed after simulating all the system components in PSIM, and consistently obtaining the desired results.

### 4.1 Hardware

The charger module is capable of charging 12V lead-acid batteries, 9.6V nickel-metal hydride batteries and 16V ultracapacitors. It is quite heavy and bulky, because a 1.5kVA, 50Hz transformer was used. So, it was decided that the charger would stay out of the mobile platform, working as a charging station. This strategy is valid, because the mobile platform is able to move itself to the charging station when recharging is needed.

The final version of the charger module was implemented on a printed circuit board (PCB). Figure 8 shows the charging of a 16V, 116F ultracapacitors module, at a reference current of 20A.

The voltage regulator module is capable of supplying a regulated 12V voltage to the mobile platform using batteries or ultracapacitors as energy sources. Its input voltage may be between 16V and, approximately, 1.5V (this lower limit is mainly used by ultracapacitors).

Figure 9 presents the voltage regulator module implemented on a PCB. The DC-DC converters diodes, MOSFETs and coils are clearly visible; the AVR ATmega 328P microcontroller from Atmel Corporation and the dedicated crystal are also noticeable. Some LEDs provide visible signals.

The voltage regulator module and its power source (batteries or ultracapacitors) are supposed to be installed on board the mobile platform, which has been done. Figure 10 shows a previously charged 16V, 116F ultracapacitors module serving as the energy source of a four-wheeled mobile platform.



Figure 8: Charger module charging a 16V, 116F ultracapacitors module at a reference current of 20A.



Figure 9: Voltage regulator module.

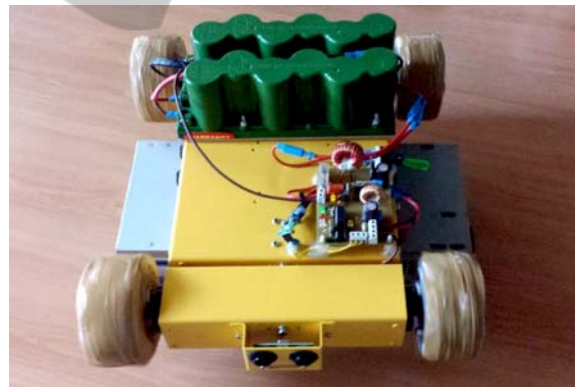


Figure 10: Voltage regulator module and a 16V, 116F ultracapacitors module installed on board a four-wheeled mobile platform. The picture was taken with a long exposure and it is noticeable that the wheels are turning.

### 4.2 Software

As mentioned before, the charger module must be capable of charging ultracapacitors and different kinds of batteries. And the voltage regulator module must provide a regulated 12V voltage to the mobile platform. The PI control algorithms of both modules were implemented on AVR ATmega 328P microcontrollers.

The operation mode of the charger module depends on the type of energy-storing device to be charged. The following algorithms have been chosen for implementation because they are the most used for each type of energy-storing device:

- The NDV (Negative Delta Voltage) for nickel-metal hydride batteries;
- Constant current followed by constant voltage for lead-acid batteries;
- Constant current until voltage reaches a predetermined value for ultracapacitors.

Regardless of the type of energy-storing device, charging time is not controllable because it depends on the characteristics of the energy-storing device and its initial state of charge.

A user-friendly interface with a LCD (Liquid Crystal Display) and some push buttons was also developed, allowing the user to select the type of energy-storing device to be charged and define charging parameters. Charging options include: type of battery; battery voltage; battery charging current; battery capacity; ultracapacitor maximum voltage and ultracapacitor charging current.

The control algorithm flowchart of the voltage regulator module is shown in Figure 11. This module is also able to detect load overcurrents and, if necessary, automatically shuts down to prevent damages to the system components.

## 5 EXPERIMENTAL RESULTS

A few experimental tests were made to the system in order to ensure the correct functioning of each module and, also, to further validate the proposed concept.

### 5.1 The Charger

The charger module was tested with three energy-storing devices:

- One 16V, 116F, 4.12Wh ultracapacitors module;
- One 12V, 12Ah, 144Wh lead-acid battery;
- One 9.6V, 800mAh, 7.68Wh nickel-metal hydride battery.

The expected autonomy of the mobile platform powered by the tested nickel-metal hydride battery after a full charge is rather low. It ranges, approximately, from 30 to 35 minutes. The purpose of using this battery is just to verify the ability of the charger to work properly with nickel-metal hydride batteries.

The results show that the maximum error

resulting from the difference between the desired value and the actual value of a battery charging current never exceeded 4%. The end-of-charge algorithm worked as expected for both types of batteries. The charging times are, approximately, 8 hours for the lead-acid battery and 4 hours for the nickel-metal hydride battery.

In ultracapacitors charging mode, the charger module imposed a current around 20A, charging the 116F ultracapacitors module up to 15V in 1 minute and 57 seconds. Since the difference between the reference current and output current never exceeded 700mA, the resulting maximum error is 3.5%.

### 5.2 The Voltage Regulator

The voltage regulator module, powered by the 116F ultracapacitors module previously charged up to 15V, was tested on the mobile platform. The tests were performed on a flat and levelled ground. Under these operating conditions, the platform absorbed, approximately, 0.8A while keeping a constant speed of 62.8cm/s. The system worked at full performance for 22 minutes. It was also found that, under the conditions described above, the voltage regulator succeeded in imposing the required output voltage of 12V until its input voltage, provided by the ultracapacitors module, dropped to about 1.5V.

Some tests with excessive overcurrents at the load were also conducted. In all tested situations, the system was able to detect the overcurrent and did shut down before the occurrence of any damage.

## 6 CONCLUSIONS AND FUTURE DEVELOPMENTS

A power supply system for a mobile robot platform has been developed. The system may use ultracapacitors, lead-acid batteries or nickel-metal hydride batteries as energy-storing devices.

It proved its ability to charge one 116F, 4.12Wh ultracapacitors module up to 15V in 1 minute and 57 seconds. The system also proved its ability to properly charge different types of batteries, following the reference current with an error less than 4%, and effectively detecting the full charge state. The algorithms used in this project for battery charging, sought to diminish charging times, but without causing significant battery deterioration.

Both simulations results and experimental results presented in this paper validate the possibility of providing the mobile robot platform with an electrical energy storage system integrating

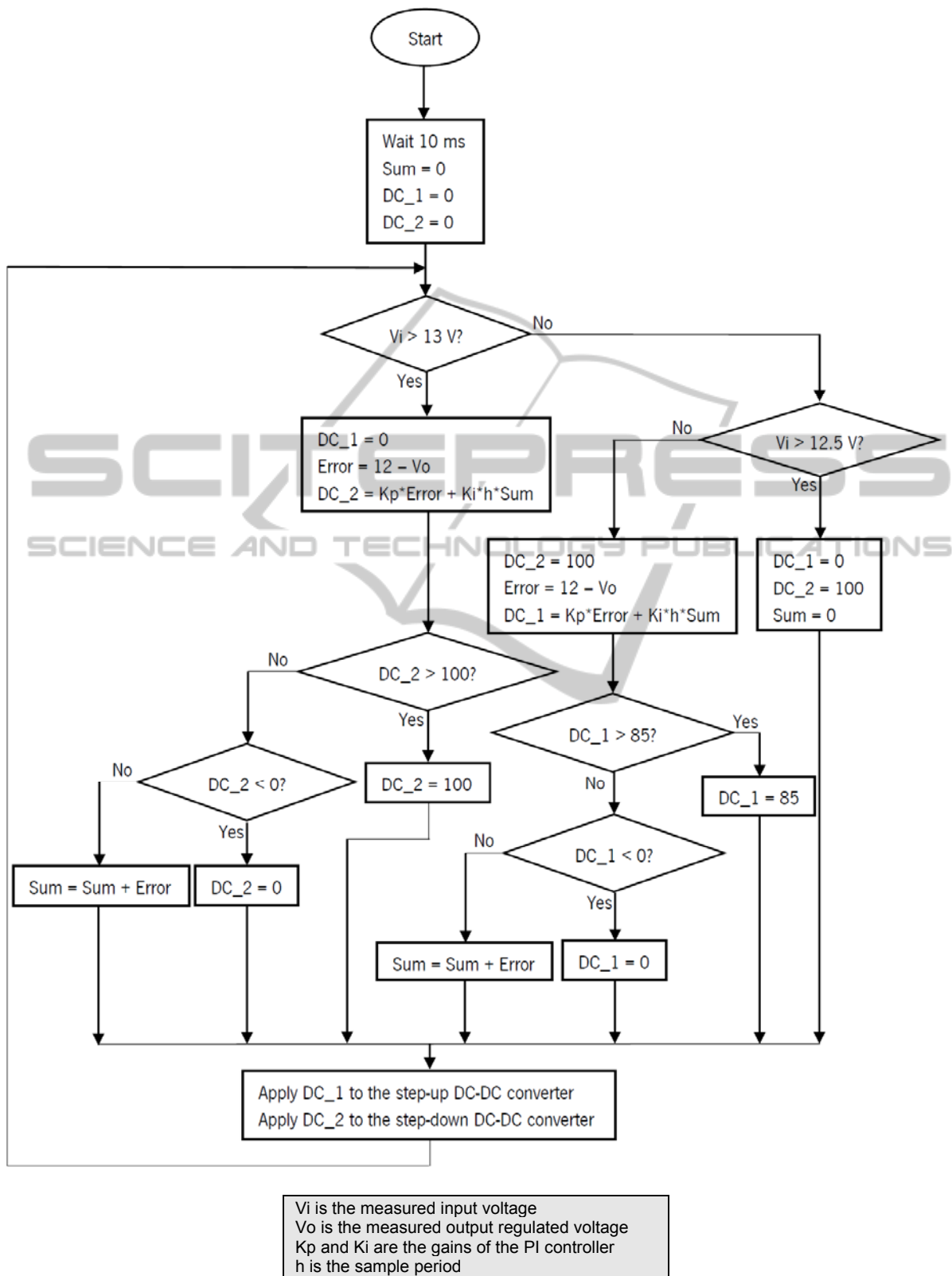


Figure 11: Control algorithm flowchart of the voltage regulator module.

ultracapacitors and batteries. Such integration, suggested as future work, would ensure both the autonomy and the charging speed requirements of the platform. In fact, using exclusively one 116F, 4.12Wh ultracapacitors module as energy-storing device, the mobile platform achieved an autonomy of 22 minutes after a charging time of 1 minute and 57 seconds, exceeding the autonomy required by the platform when the charging time is limited to 2 minutes. It should be noted that the charging time is less than 10% of the autonomy time. On the other hand, the expected autonomy of the mobile platform powered by a fully charged conventional 12V, 12Ah, 144Wh lead-acid battery, like the one used in this work, ranges from 7 to 9 hours, fully satisfying the autonomy required by the platform when there are no charging time restrictions.

Integrating ultracapacitors and batteries in the same power supply system also would release the batteries from the requirement of providing high power peaks, extending their lifetime.

Battery energy densities are much larger than the ones offered by ultracapacitors but the introduction of new materials may reduce the difference in a near future.

An ultracapacitor is much more expensive than a battery with the same energy storage capacity. However, ultracapacitors cost has been significantly decreasing. Furthermore, because ultracapacitors allow much more charging/discharging cycles than batteries, the cost difference between the two components is mitigated.

In addition to the suggested integration of ultracapacitors and batteries in the same power supply system, the following tasks are suggested as future work: implementing control algorithms capable of identifying the battery type to be charged and its voltage; using a high-frequency transformer instead of a 50Hz transformer, which would reduce the cost, size and weight of the charger module, allowing its installation onboard the mobile platform; developing more compact PCBs using surface-mount devices (SMD).

## ACKNOWLEDGEMENTS

This work has been supported by FCT – Fundação para a Ciência e Tecnologia within the Project Scope: Pest-OE/EEI/UI0319/2014.

## REFERENCES

- Awerbuch, J. J.; Sullivan, C. R.; Control of Ultracapacitor-Battery Hybrid Power Source for Vehicular Applications; *ENERGY 2008, Energy 2030 Conference*, 2008, Page(s): 1 – 7. Digital Object Identifier: 10.1109/ENERGY.2008.4781003.
- Awerbuch, J. J.; Sullivan, C. R.; Filter-based Power Splitting in Ultracapacitor-Battery Hybrids for Vehicular Applications; *COMPEL 2010, Control and Modeling for Power Electronics*, 2010, Pages(s): 1 – 8. Digital Object Identifier: 10.1109/COMPEL.2010.5562429.
- Bernholc, J.; Ranjan, V.; Zheng, X. H.; Jiang, J.; Lu, W.; Abtew, T. A.; Boguslawski, P.; Nardelli, M.B.; Meunier, V.; Properties of High-Performance Capacitor Materials and Nanoscale Electronic Devices, *HPCMP-UGC 2010, High Performance Computing Modernization Program Users Group Conference*, 2010, Page(s): 195 – 200. Digital Object Identifier: 10.1109/HPCMP-UGC.2010.76.
- Dai Haifeng; Chang Xueyu; A Study on Lead Acid Battery and Ultra-capacitor Hybrid Energy Storage System for Hybrid City Bus; *ICOIP 2010, International Conference on Optoelectronics and Image Processing*, 2010, Page(s): 154 – 159. Digital Object Identifier: 10.1109/ICOIP.2010.321.
- Haihua Zhou; Bhattacharya, T.; Duong Tran; Siew, T. S. T.; Khambadkone, A. M.; Composite Energy Storage System Involving Battery and Ultracapacitor With Dynamic Energy Management in Microgrid Applications; *IEEE Transactions on Power Electronics*, 2010, Page(s): 923 – 930. Digital Object Identifier: 10.1109/TPEL.2010.2095040.
- Hua, A. C. -C.; Syue, B. Z. -W.; Charge and discharge characteristics of lead-acid battery and LiFePO4 battery; *IPEC 2010, International Power Electronics Conference*, 2010, Page(s): 1478 – 1483. Digital Object Identifier: 10.1109/IPEC.2010.5544506.
- JennHwa Wong; Idris, N. R. N.; Anwari, M.; Taufik, T.; A Parallel Energy-Sharing Control for Fuel cell-Battery-Ultracapacitor Hybrid Vehicle; *ECCE 2011, Energy Conversion Congress and Exposition*, 2011, Page(s): 2923 – 2929. Digital Object Identifier: 10.1109/ECCE.2011.6064162.
- Lei Wang; Hui Li; Maximum Fuel Economy-oriented Power Management Design for a Fuel Cell Vehicle Using Battery and Ultracapacitor; *IEEE Transactions on Industry Applications*, 2010, Page(s): 1011 – 1020. Digital Object Identifier: 10.1109/TIA.2010.2045097.
- Li Siguang; Zhang Chengning; Xie Shaobo; Research on Fast Charge Method for Lead-Acid Electric Vehicle Batteries; *ISA 2009, International Workshop on Intelligent Systems and Applications*, 2009, Page(s): 1 – 5. Digital Object Identifier: 10.1109/IWISA.2009.5073068.
- Miller, J. M.; Energy Storage Technology Markets and Application's: Ultracapacitors in Combination with Lithium-ion; *ICPE 2007, International Conference on*

- Power Electronics*, 2007, Page(s): 16 – 22. Digital Object Identifier: 10.1109/ICPE.2007.4692343.
- Monteiro, J.; Garrido, N.; Fonseca, R.; Efficient Supercapacitor Energy Usage in Mobile Phones; *ICCE 2011, 2011 International Conference on Consumer Electronics* – Berlin, 2011, Pages(s): 318 – 321. Digital Object Identifier: 10.1109/ICCE-Berlin.2011.6031796.
- Musat, A. M.; Carp, M.; Borza, P.; Musat, R.; Sojref, D.; Hybrid Storage Systems and Dynamic Adapting Topologies for Vehicle Applications; *OPTIM 2012, 2012 13th International Conference on Optimization of Electrical and Electronic Equipment*, 2012, Page(s): 1842 – 1566. Digital Object Identifier: 10.1109/OPTIM.2012.6231910.
- Niemoeller, B. A.; Krein, P. T.; Battery-Ultracapacitor Active Parallel Interface with Indirect Control of Battery Current; *PECI 2010, Power and Energy Conference at Illinois*, 2010, Pages(s): 12 – 19. Digital Object Identifier: 10.1109/PECI.2010.5437163.
- Petchjaturorn, P.; Wicheanchote, P.; Khaehintung, N.; Kiranon, W.; Sunat, K.; Chiewchanwattana, S.; Intelligent ultra fast charger for Ni-Cd batteries; *ISCAS 2005, IEEE International Symposium on Circuits and Systems*, 2005, Page(s): 5162 - 5165 Vol. 5. Digital Object Identifier: 10.1109/ISCAS.2005.1465797.
- Schneuwly, A.; Gallay, R.; Properties and Applications of Supercapacitors from the State-of-Art to Future Trends; *Proceeding PCIM 2000*, 2000.
- Wenzhong Gao; Performance Comparison of a Fuel Cell-Battery Hybrid Powertrain and a Fuel Cell-Ultracapacitor Hybrid Powertrain; *IEEE Transactions On Vehicular Technology*, 2005, Page(s): 846 – 855. Digital Object Identifier: 10.1109/TVT.2005.847229.
- Xiaofei Liu; Qianfan Zhang; Chunbo Zhu; Design of Battery and Ultracapacitor Multiple Energy Storage in Hybrid Electric Vehicle; *VPPC 2009, Vehicle Power and Propulsion Conference*, 2009, Page(s): 1395 – 1398. Digital Object Identifier: 10.1109/VPPC.2009.5289462.